Repeated enrichment of trace metals and organic carbon on an Eocene high-energy shelf caused by anoxia and reworking

Publisher: GSA
Journal: GEOL: Geology
DOI:10.1130/G38412.1

Repeated enrichment of trace metals and organic carbon on an Eocene high energy shelf caused by anoxia and reworking

Christian März[1,2*], T. Wagner[1,3] S. Aqleh[1], M. Al-Alaween[1], S. van den Boorn[4], O.G. Podlaha[4], S. Kolonic[5], S.W. Poulton[2], B. Schnetger[6], and H.-J. Brumsack[6]

[1]*School of Civil Engineering and Geosciences, Newcastle University, UK*

[2]*School of Earth and Environment, University of Leeds, UK*

[3]*Lyell Centre, Heriot-Watt University, Edinburgh, UK*

[4]*Shell Global Solutions International B.V., Projects and Technology, Rijswijk, The Netherlands*

[5]*Shell Petroleum Development Company of Nigeria Ltd, Nigeria*

[6]*ICBM, University of Oldenburg, Germany*

*E-mail: c.maerz@leeds.ac.uk

ABSTRACT

Petroleum source rocks are strongly enriched in organic carbon (OC), and their trace metal (TM) contents often reach low grade ore levels. The mechanisms leading to these co-enrichments are important for understanding how extreme environmental conditions support the formation of natural resources. We therefore studied organic-rich Eocene marls and limestones (oil shale) from the central Jordan Amzaq-Hazra sub-basin, part of a Cretaceous-Paleogene shelf system along the southern Neo-Tethys margin. Geochemical analyses on two cores show highly dynamic depositional conditions, consistent with sedimentological and micropaleontological observations. Maximum and

Publisher: GSA
Journal: GEOL: Geology
DOI:10.1130/G38412.1

average contents in OC (~26 and ~10 wt%), S (~7 and ~2.4 wt%), P (~10 and ~2 wt%), Mo (>400 and ~130 ppm), Cr (>500 and ~350 ppm), V (>1,600 and ~550 ppm) and Zn (>3,800 and ~900 ppm) are exceptional, in particular without any indication of hydrothermal or epigenetic processes. We propose a combination of two processes: Physical reworking of OC- and metal-rich material from locally exposed Cretaceous-Paleogene sediments (as supported by re-worked nannofossils); and high marine productivity fueled by chemical remobilization of nutrients and metals on land that sustained anoxic-sulfidic conditions. Burial of high-quality organic matter (Hydrogen Index 600–700 mgHC/gOC) was related to strongly reducing conditions, punctuated by only short-lived oxygenation events, and to excess H_2S promoting organic matter sulphurisation. These processes likely caused the OC/TM co-enrichments in a high-energy shallow marine setting that contradicts common models for black shale formation, but may explain similar geochemical patterns in other black shales.

INTRODUCTION

Marine shales rich in organic carbon (OC) and trace metals (TMs) represent extreme environmental conditions under perturbed biogeochemical cycles in the geological pas. High primary productivity and anoxic/sulfidic redox conditions are particularly conducive to their formation (Brumsack, 1980; Demaison and Moore, 1980). Metal enrichments reaching low ore grade in black shales (Anjum et al., 2012) are typically explained by secondary enrichment via metal-rich hydrothermal fluids or brines (Eugster, 1985; Coveney and Glascock, 1989; Lehmann et al., 2007). Understanding these processes is important to gain insight into extreme states of Earth's climate system, and the formation and potential location of hydrocarbon and metal resources. To address

the topic of paired OC/TM enrichments, we applied geochemical analyses coupled with sedimentological observations to Eocene, thermally immature OC-rich sediments ('oil shale') from two wells in central Jordan. This region was part of an extended paleo-shelf system throughout the Cretaceous-Paleogene, with numerous tectonically induced sub-basins (Alqudah et al., 2015) covering large parts of the Arabian-African margins of the Neo-Tethys (Fig. 1).

METHODS

The oil shale interval in cores OS22 and OS23 from central Jordan is ~225 m thick (Fig. 1). Lithological units A and C are heterogeneous marls, phosphates, cherts and limestones; unit B is more homogenous with interbedded laminated marls (Ali Hussein et al., 2014a). The oil shale succession is part of the Umm Rijam Chalk Limestone Formation, deposited across the Early-Middle Eocene (Ypresian-Lutetian) Amzaq-Hazra sub-basin (Alqudah et al., 2014a, 2015). 186 samples were selected for geochemical analysis. Total sulfur (S), total organic carbon (OC) and carbonate (calculated as $CaCO_3$) were determined by Leco combustion analysis. The Hydrogen Index (HI) was analyzed with a Rock Eval 6 analyzer. X-Ray Fluorescence (XRF) analysis was used to quantify major (Al, Fe, P) and trace (Cr, Mo, V, Zn, Zr) element contents. TM excess contents ($element_{xs}$) (Brumsack, 2006) were calculated relative to element/Al ratios of average shale (Wedepohl, 1991). Sequential Fe (Poulton and Canfield, 2005) and chromium-reducible S (CRS) extractions (Canfield et al., 1986) were used to calculate the ratios of highly reactive to total Fe (FeHR/FeT), and of sulfide-bound to highly reactive Fe (FeS/FeHR). Data are displayed against "adjusted depth" with zero depth (0 m) defined

Publisher: GSA
Journal: GEOL: Geology
DOI:10.1130/G38412.1

as top of the oil shale interval. As both cores exhibit the same geochemical patterns, only OS23 data are displayed in Figure 2 (for OS22, see Electronic Supplement).

RESULTS

The cores are subdivided into geochemical Units I to V (Fig. 2). Units I+II, III and IV+V correlate with lithological units A, B and C (Ali Hussein et al., 2014a). Units II and IV are geochemically more variable than the rather uniform Units I, III and V. The sediment is dominantly composed of $CaCO_3$ (av. ~60 wt%) and TOC (av. ~10 wt%) with high amplitude and high frequency variability (Fig. 2). Both S and P are enriched in parts of the records (up to ~7 and ~10 wt%, respectively), with S showing a very strong relationship with OC ($R^2 > 0.95$), while Al contents of ~0.1 to ~3.6 wt% (av. ~1.0 wt%) indicate very little fine-grained siliciclastic material (Fig. 2A). Throughout the record, OC is of excellent quality (kerogen type I/IIS), with Hydrogen Indices (HI) of 600–700 mgHC/gOC that do not match the OC fluctuations (Fig. 2A). Extreme enrichments of Mo, Cr, V and Zn occur in Units II and IV (Fig. 2B), and to a lesser extent in Units I, III and V, as evident from average excess contents (Table 1, Fig. DR1). Iron and S speciation data indicate that > 80% of the S is bound to OC (Fig. 2B). High FeHR/FeT ratios > 0.38 suggest anoxic bottom waters throughout the section, while fluctuations in FeS/FeHR ratios around 0.7 indicate oscillations between sulfidic and non-sulfidic water column conditions (Poulton and Canfield, 2011).

DISCUSSION

Our data provide intriguing insights into the depositional environment of the Jordan oil shales. Units I, III and V tend to have FeS/FeHR ratios below 0.7 (Fig. 2B). However, the observed ratios of ~0.6 are nevertheless quite high (Poulton and Canfield,

Publisher: GSA
Journal: GEOL: Geology
DOI:10.1130/G38412.1

2011) and, when considered alongside significant TM enrichments (Figs. 2A, DR1, Table 1), indicate an anoxic water column during deposition of Units III and V, likely fluctuating between sulfidic and non-sulfidic conditions. With no evidence for oxic conditions, these laminated and rather homogenous Units likely document quiet sedimentation under stable anoxia. This is supported by negative correlations between OC and biogenic $CaCO_3$ in Unit III in both cores (R^2 = 0.48 and 0.76), implying dilution of organic material by biogenic carbonate under steady hemi-pelagic sedimentation (Alqudah et al., 2014a, b).

In contrast, Units II and especially IV show very different characteristics (Fig. 2). High TM enrichments, in particular Mo, combined with Fe and S speciation data strongly argue for at least episodically sulfidic bottom waters (Brumsack, 1980, 2006; Poulton and Canfield, 2011). In support of this, high amounts of non-sulphide S and the occurrence of Mo/Al peaks at maximum OC (Fig. 2) suggest that kerogen type I/IIS preservation was favored by OM sulfurization due to excess H_2S availability relative to highly reactive Fe (Tribovillard et al., 2004, 2015). However, the TM records (Fig. 2B) also suggest significant redox variability during deposition of Units II and IV. Peaks in Zr and P (Fig. 2B) indicate a dynamic setting with episodically high depositional energies, probably induced by currents and/or wave action enriching heavy minerals like zircon and apatite (März et al., 2011). In agreement with convoluted and tilted bedding, tempestites, and intensely bioturbated horizons in Units II and IV, this suggests deposition above the storm or even fair weather wave base (Ali Hussein et al., 2014a, b). These observations suggest extreme redox variability, from sulfidic water column conditions through to high-energy oxic periods with mixing and ventilation. Such conditions are commonly regarded

Publisher: GSA
Journal: GEOL: Geology
DOI:10.1130/G38412.1

as unfavorable for the preservation of high-quality kerogen, as ventilation should lead to partial OC degradation (Demaison and Moore, 1980; Hedges and Keil, 1995).

Within this context it is notable that excess Mo, U, V, Zn, Ni and Cr for Units II, III and IV exceed those of modern organic-rich deposits (the permanently sulfidic Black Sea, and the episodically sulfidic Peru upwelling area. They are, however, comparable to Cretaceous Oceanic Anoxic Event 2 sediments documenting widespread, long-lasting anoxia/euxinia (Brumsack, 2006), and to the Cretaceous-Paleogene Belqa Group deposits (Table 1, Fig. DR1) exposed near the coring sites in Jordan (Fleurance et al., 2013). Finally, the Eocene TM patterns show similarities to metalliferous Cambrian (Lehmann et al., 2007) and Carboniferous shales (Coveney and Glascock, 1989; Slack et al., 2015) (Fig. DR1). For the latter, syn- or epigenetic hydrothermal input has been suggested as the dominant TM source (Coveney and Glascock, 1989). Lithological and geochemical properties of the Jordan shale (e.g., well-preserved sedimentary features, low thermal maturity), however, support neither a sedimentary exhalative (SEDEX-type) mechanism nor any post-depositional, epigenetic intrusion of metal-rich solutions (see Electronic Supplement).

We instead propose that there were two key factors for TM enrichments and for high quality OC production and preservation in the Eocene Jordan shales (Fig. 3): (1) The water column was anoxic to euxinic during deposition of Units II, III and IV due to high primary productivity and semi-restriction of the depositional basins (Demaison and Moore, 1980; Alqudah et al., 2014a, b). (2) Different from interpretations of most black shale deposits, the Eocene Jordan shale received material physically eroded and/or chemically weathered from OC- and TM-rich Cretaceous-Paleocene limestones, marls

and shales exposed in proximal/transitional settings close to the study sites (Fleurance et al., 2013). During the Cretaceous to Eocene, active tectonic processes (Alqudah et al., 2014 a, b) favored re-distribution of erosional products from older strata across the shelf, especially during periods of low relative sea level and high depositional energy, where this material was mixed with autochthonous deposits. Alternative to, or in combination with, physical re-distribution, chemical weathering of local OM- and TM-rich rocks could have provided excess nutrients to the Eocene basin, enhancing primary productivity particularly under the warm and humid Eocene climate (Pearson et al., 2007).

Evidence for physical erosion comes from the high abundance (sometimes dominance) of re-worked Cretaceous to Eocene nannofossils in the cores studied (Alqudah et al., 2014a, b) (Fig. 1). Localized tectonic processes causing syn-sedimentary uplift and exposure of older sediments along the horst structures bordering the Amzaq-Hazra sub-basin supported intense current- or wave-driven erosion events (Alqudah et al., 2014a, b). This process would have resulted in re-deposition of older OC- and TM-rich material, accompanied by drawdown of water column TMs and preservation of OC under high primary productivity and sulfidic water column conditions (Fig. 3). Chemical weathering and/or physical erosion of OC-, TM- and nutrient-rich lithologies exposed on land might have contributed to increased nutrient supply, higher productivity, and ultimately the OC/TM co-enrichment in the Eocene shale basins. However, weathering and transport under oxic conditions would have partly degraded the organic matter before it entered the anoxic/sulfidic shelf waters, which is inconsistent with the high kerogen quality throughout the studied sediments. We therefore assume that input from land was

secondary to wave- and current-induced re-distribution processes on an anoxic/sulfidic shelf (Baird and Brett, 1991).

Irrespective of the transport pathways of eroded material, reworking of Cretaceous-Paleocene strata was variable but generally persistent throughout large parts of the Jordan oil shale deposition (Alqudah et al., 2014a) (Fig. 1). The low-energy conditions prevailing during deposition of Unit III should have favored lateral advection of fine and fragile calcareous coccoliths, clay minerals, and associated OM. The lower percentage of reworked nannofossils in parts of Units II and IV does not exclude that erosion and reworking took place, but suggests that the fine material was winnowed away, leaving only coarser/denser particles (rich in Zr, P and Cr) to settle and accumulate (Fig. 3). It appears reasonable that a significant fraction of OC and TM in the sediment may derive from this hydrodynamically sorted material. Similar processes have been described for Paleozoic black shales (Baird and Brett, 1991; Formolo and Lyons, 2007), highlighting the potential role of submarine erosion and re-working on anoxic high-energy shelves in generating TM/OC enrichments. The variability in current and wave intensity and continental export was probably linked to Eocene subtropical trade wind dynamics, with alternations between periods of aridity (stronger winds, shelf reworking) and humidity (weaker winds, continental export) (Huber and Goldner, 2012).

While this study describes environmental conditions and reworking processes for one Eocene sub-basin of the Neo-Tethys shelf, it also confirms that OC- and TM-enriched intervals are tens of meters thick in two cores drilled ~10 km apart, with synchronous oil shale deposits spreading over ~100 km across the Amzaq-Hazra sub-basin (Alqudah et al., 2015). We suggest that similar processes were active across large

parts of the Eocene Neo-Tethys shelf, and may also have operated during other periods of widespread black shale deposition that occurred under similar environmental and tectonic conditions. A notable example of OC/TM co-enrichment comparable to the Jordan shale is a ~7 m thick Eocene black shale succession from the Central Arctic Lomonosov Ridge. This interval is characterized by variable but partly high enrichments in OC, S and metals (including Fe, Cr, Mo, Zn), indicative of at least episodically anoxic/sulfidic bottom waters (Sangiorgi et al., 2008; März et al., 2011). But geochemical and mineralogical proxies also support a dynamic setting with high depositional energies and very low sedimentation rates in shallow waters (März et al., 2011). By analogy to the Jordan setting, we suggest that chemical re-mobilization and/or physical erosion and reworking of Cretaceous-Paleocene black shales on the Lomonosov Ridge contributed to the observed element records. Black shale deposits from Mesozoic shallow water systems also show features consistent with those reported from the Eocene Jordan shelf. Petrographic and geochemical analyses of lower Toarcian black shales of the Posidonia Shale Formation in the Dutch Central Graben (Trabucho-Alexandre et al., 2012), for example, support dynamic energetic conditions driven by intense and variable bottom currents as key controls on shale deposition, rather than vertical settling alone.

CONCLUSIONS

Based on geochemical data from two Eocene oil shale intervals in Jordan, we present a model explaining high OC and TM enrichments in a shelf basin along the southern margin of the Western Tethys. Critical factors are (1) overall high marine productivity promoting anoxic/sulfidic water column conditions and OM sulphurisation, and (2) the re-distribution of OM- and TM-rich deposits of Cretaceous-Paleogene age

from the inner shelf and hinterland. These factors, with a dominance of current- and wave-induced reworking on the shelf, were strongly favored by the prevailing tectonic regime, including small-scale extensional tectonics that generated semi-restricted shelf basins in graben structures. Similar processes were likely active across large parts of the Cretaceous-Paleogene Levantine shelf basins, and they should also be considered for widespread shale deposits that formed under comparable paleo-environmental conditions in tectonically active settings. This study challenges the common perception of stagnant ('non-dynamic') depositional conditions during marine black shale formation. Instead, it shifts the focus to dynamic, high-energy and tectonically active paleo-settings where multiple climatic, depositional and tectonic processes overlap to produce extreme geochemical shale properties. With this scope, our study also provides links to low-grade ore resources generated without any syn- or post-depositional hydrothermal activity.

ACKNOWLEDGMENTS

Substantial financial and analytical support for this project from Shell Global Solutions and JOSCo is gratefully acknowledged. We are indebted to C. Lehners, E. Gruendken and for P. Green for assistance with sample preparation and analysis, and to M. Ali Hussein and M. Alqudah for fruitful discussions. N. Tribovillard, P. Meyers and an anonymous reviewer provided insightful comments on an earlier version of the manuscript.

REFERENCES CITED

Ali Hussein, M., Alqudah, M., Van den Boorn, S., Kolonic, S., Podlaha, O.G., and Mutterlose, J., 2014a, Eocene oil shales from Jordan – their petrography, carbon and oxygen stable isotopes: GeoArabia, v. 19, p. 139–162.

Ali Hussein, M., Alqudah, M., Podlaha, O.G., Van den Boorn, S., Kolonic, S., and Mutterlose, J., 2014b, Ichnofabrics of Eocene oil shales from central Jordan and their use for paleoenvironmental reconstructions: GeoArabia, v. 19, p. 145–160.

Alqudah, M., Ali Hussein, M., Podlaha, O.G., Van den Boorn, S., Kolonic, S., and Mutterlose, J., 2014a, Calcareous nannofossil biostratigraphy of Eocene oil shales from central Jordan: GeoArabia, v. 19, p. 117–140.

Alqudah, M., Ali Hussein, M., Van den Boorn, S., Giraldo, V.M., Kolonic, S., Podlaha, O.G., and Mutterlose, J., 2014b, Eocene oil shales from Jordan - paleoenvironmental implications from reworked microfossils: Marine and Petroleum Geology, v. 52, p. 93–106, doi:10.1016/j.marpetgeo.2014.02.001.

Alqudah, M., Ali Hussein, M., Van den Boorn, S., Podlaha, O.G., and Mutterlose, J., 2015, Biostratigraphy and depositional setting of Maastrichtian e Eocene oil shales from Jordan: Marine and Petroleum Geology, v. 60, p. 87–104.

Anjum, F., Shahid, M., and Akcil, A., 2012, Biohydrometallurgy techniques of low grade ores: a review on black shales: Hydrometallurgy, v. 117–118, p. 1–12, doi:10.1016/j.hydromet.2012.01.007.

Baird, G.C., and Brett, C.E., 1991, Submarine erosion on the anoxic sea floor: Stratinomic, paleoenvironmental, and temporal significance of reworked pyrite-bone deposits, *in* Tyson, R.V., and Pearson, T.H., eds., Modern and Ancient Continental Shelf Anoxia: Geological Society Special Publication 58, p. 233–257, doi:10.1144/GSL.SP.1991.058.01.16.

249 Brumsack, H.-J., 1980, Geochemistry of Cretaceous black shales from the Atlantic Ocean
250 (DSDP Legs 11, 14, 36 and 41): Chemical Geology, v. 31, p. 1–25,
251 doi:10.1016/0009-2541(80)90064-9.
252 Brumsack, H.-J., 2006, The trace metal content of recent organic carbon-rich sediments:
253 implication for Cretaceous black shale formation: Palaeogeography,
254 Palaeoclimatology, Palaeoecology, v. 232, p. 344–361,
255 doi:10.1016/j.palaeo.2005.05.011.
256 Canfield, D.E., Raiswell, R., Westrich, J.T., Reaves, C.M., and Berner, R.A., 1986, The
257 use of chromium reduction in the analysis of reduced inorganic sulphur in sediments
258 and shales: Chemical Geology, v. 54, p. 149–155, doi:10.1016/0009-2541(86)90078-
259 1.
260 Coveney, R.M., and Glascock, M.D., 1989, A review of the origins of metal-rich
261 Pennsylvanian black shales, central U.S.A., with an inferred role for basinal brines:
262 Applied Geochemistry, v. 4, p. 347–367, doi:10.1016/0883-2927(89)90012-7.
263 Demaison, G.J., and Moore, G.T., 1980, Anoxic environments and oil source bed
264 genesis: Organic Geochemistry, v. 2, p. 9–31, doi:10.1016/0146-6380(80)90017-0.
265 Eugster, H.P., 1985, Oil shales, evaporates and ore deposits: Geochimica et
266 Cosmochimica Acta, v. 49, p. 619–635, doi:10.1016/0016-7037(85)90158-9.
267 Fleurance, S., Cuney, M., Malartre, F., and Reyx, J., 2013, Origin of the extreme
268 polymetallic enrichment (Cd, Cr, Mo, Ni, U, V, Zn) of the Late Cretaceous-Early
269 Tertiary Belqa Group, central Jordan: Palaeogeography, Palaeoclimatology,
270 Palaeoecology, v. 369, p. 201–219, doi:10.1016/j.palaeo.2012.10.020.

Formolo, M.J., and Lyons, T.W., 2007, Accumulation and preservation of reworked marine pyrite beneath an oxygen-rich Devonian atmosphere: constraints from sulfur isotopes and framboid textures: Journal of Sedimentary Research, v. 77, p. 623–633, doi:10.2110/jsr.2007.062.

Hedges, J.I., and Keil, R.G., 1995, Sedimentary organic matter preservation: An assessment and speculative synthesis: Marine Chemistry, v. 49, p. 81–115, doi:10.1016/0304-4203(95)00008-F.

Huber, M., and Goldner, A., 2012, Eocene monsoons: Journal of Asian Earth Sciences, v. 44, p. 3–23, doi:10.1016/j.jseaes.2011.09.014.

Lehmann, B., Nägler, T.F., Holland, H.D., Wille, M., Mao, J.W., Pan, J.Y., Ma, D.S., and Dulski, P., 2007, Highly metalliferous carbonaceous shale and Early Cambrian seawater: Geology, v. 35, p. 403–406, doi:10.1130/G23543A.1.

März, C., Vogt, C., Schnetger, B., and Brumsack, H.-J., 2011, Variable Eocene-Miocene sedimentation processes and bottom water redox conditions in the Central Arctic Ocean (IODP Expedition 302): Earth and Planetary Science Letters, v. 310, p. 526–537, doi:10.1016/j.epsl.2011.08.025.

Pearson, P.N., Van Dongen, B.E., Nicholas, C.J., Pancost, R.D., Schouten, S., Singano, J.M., and Wade, B.S., 2007, Stable warm tropical climate through the Eocene epoch: Geology, v. 35, p. 211–214, doi:10.1130/G23175A.1.

Poulton, S.W., and Canfield, D.E., 2005, Development of a sequential extraction procedure for iron: implications for iron partitioning in continentally derived particulates: Chemical Geology, v. 214, p. 209–221, doi:10.1016/j.chemgeo.2004.09.003.

Poulton, S.W., and Canfield, D.E., 2011, Ferruginous conditions; a dominant feature of the ocean through Earth's history: Elements, v. 7, p. 107–112, doi:10.2113/gselements.7.2.107.

Sangiorgi, F., Brumsack, H.-J., Willard, D.A., Schouten, S., Stickley, C.E., O'Regan, M., Reichart, G.-J., Sinninghe Damsté, J.S., and Brinkhuis, H., 2008, A 26 million year gap in the Central Arctic record at the greenhouse-icehouse transition: looking for clues: Paleoceanography, v. 23, PA1S04, doi:10.1029/2007PA001477.

Slack, J.F., Selby, D., and Dumoulin, J.A., 2015, Hydrothermal. Biogenic, and seawater components in metalliferous black shales of the Brooks Range, Alaska: Synsedimentary metal enrichment in a carbonate ramp setting: Economic Geology and the Bulletin of the Society of Economic Geologists, v. 110, p. 653–675, doi:10.2113/econgeo.110.3.653.

Trabucho-Alexandre, J., Dirkx, R., Veld, H., Klaver, G., Poppe, L., and de Boer, P.L., 2012, Toarcian black shales in the Dutch central graben: record of energetic, variable depositional conditions during an oceanic anoxic event: Journal of Sedimentary Research, v. 82, p. 104–120, doi:10.2110/jsr.2012.5.

Tribovillard, N., Riboulleau, A., Lyons, T., and Baudin, F., 2004, Enhanced trapping of molybdenum by sulfurized marine organic matter of marine origin in Mesozoic limestones and shales: Chemical Geology, v. 213, p. 385–401, doi:10.1016/j.chemgeo.2004.08.011.

Tribovillard, N., Haten, E., Averbuch, O., Barbecot, F., Bout-Roumazeilles, V., and Trentesaux, A., 2015, Iron availability as a dominant control on the primary

composition and diagenetic overprint of organic-matter-rich rocks: Chemical Geology, v. 401, p. 67–82, doi:10.1016/j.chemgeo.2015.02.026.

Wedepohl, K.H., 1991, The composition of the upper earth's crust and the natural cycles of selected metals. Metals in natural raw materials, *in* Merian, E., ed., Natural Resources, Metals and Their Compounds in the Environment: Weinheim, VCH, p. 3–17.

FIGURE CAPTIONS

Figure 1. A: Paleogeographic map of Paleogene Neo-Tethys, with core location on the shallow continental shelf. B: Close-up of southern Neo-Tethys margin, with location of core locations and border of present-day Jordan (after Alqudah et al., 2014b) C: Lithostratigraphic columns of cores OS23 and OS22 with sediment age, coring depth, percentages of reworked Eocene-Cretaceous calcareous nannofossils, and bioturbated intervals (after Ali Hussein et al., 2014b).

Figure 2. Core OS23 records of (A) $CaCO_3$ (wt%), Al (wt%), TOC (wt%), S (wt%), P/Al (wt%/wt%), and Zr/Al (wt%/ppm); and (B) Mo/Al (ppm/wt%), Zn/Al (ppm/wt%), V/Al (ppm/wt%), Cr/Al (ppm/wt%), FeHR/FeT, FeS/FeHR and non-sulphide S (% of total S), against adjusted drilling depth (meters, 0 m = top of black shale succession). Columns on right are geochemical Units (I-V) and lithological units (A-C).

Publisher: GSA
Journal: GEOL: Geology
DOI:10.1130/G38412.1

Figure 3. Schematic illustration of depositional conditions during deposition of Unit III, and Units II + IV (anoxic/euxinic and oxic states). Black arrows = input of OC- and TM-rich Cretaceous-Paleogene detritus. Grey arrows = input of OC- and TM-rich matter from overlying water column.

[1]GSA Data Repository item 2016xxx, xxxxxxxx, is available online at http://www.geosociety.org/pubs/ft2016.htm or on request from editing@geosociety.org.

TABLE 1. AVERAGE Mo, Cr, V, AND Zn EXCESS CONTENTS (ppm) RELATIVE TO AVERAGE SHALE COMPOSITION (WEDEPOHL, 1991) IN UNITS I TO V OF CORES OS22 AND OS23, CRETACEOUS-PALEOGENE BELQA GROUP SHALES AND LIMESTONES (FLEURANCE ET AL., 2013), BLACK SEA UNIT 2, MEDITERRANEAN SAPROPELS, AND OCEAN ANOXIC EVENT 2 DEPOSITS (BRUMSACK, 2006)

	Unit I (OS23 / OS22)	Unit II (OS23 / OS22)	Unit III (OS23 / OS22)	Unit IV (OS23 / OS22)	Unit V (OS23 / OS22)	Belqa Group[1] (shale)	Belqa Group[1] (limestone)	Black Sea[2] (Unit 2)	Med. Sapropels[2]	C/T Boundary (OAE 2)[2]
Mo_{xs} (ppm, mean)	31 / 31	97 / 104	110 / 76	401 / 272	38 / 7	496	5	116	104	315
Cr_{xs} (ppm, mean)	248 / 210	265 / 296	360 / 373	514 / 490	186 / 222	392	125	12	69	124
V_{xs} (ppm, mean)	202 / 186	608 / 501	356 / 274	1638 / 1044	139 / 129	688	113	126	457	935
Zn_{xs} (ppm, mean)	521 / 566	703 / 958	825 / 671	1906 / 469	165 / 254	4666	220	31	51	1997

Figure 1

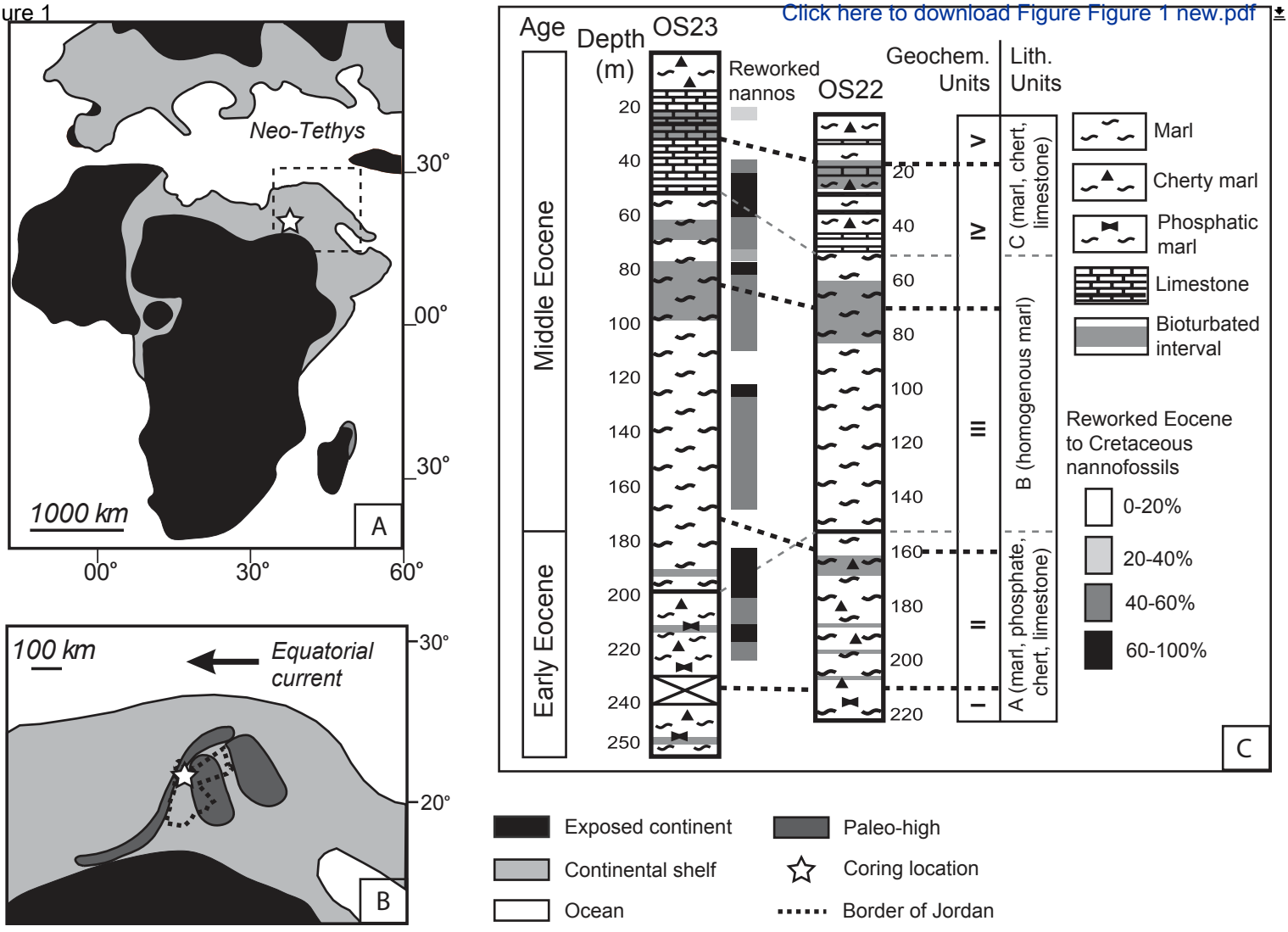

Figure 1

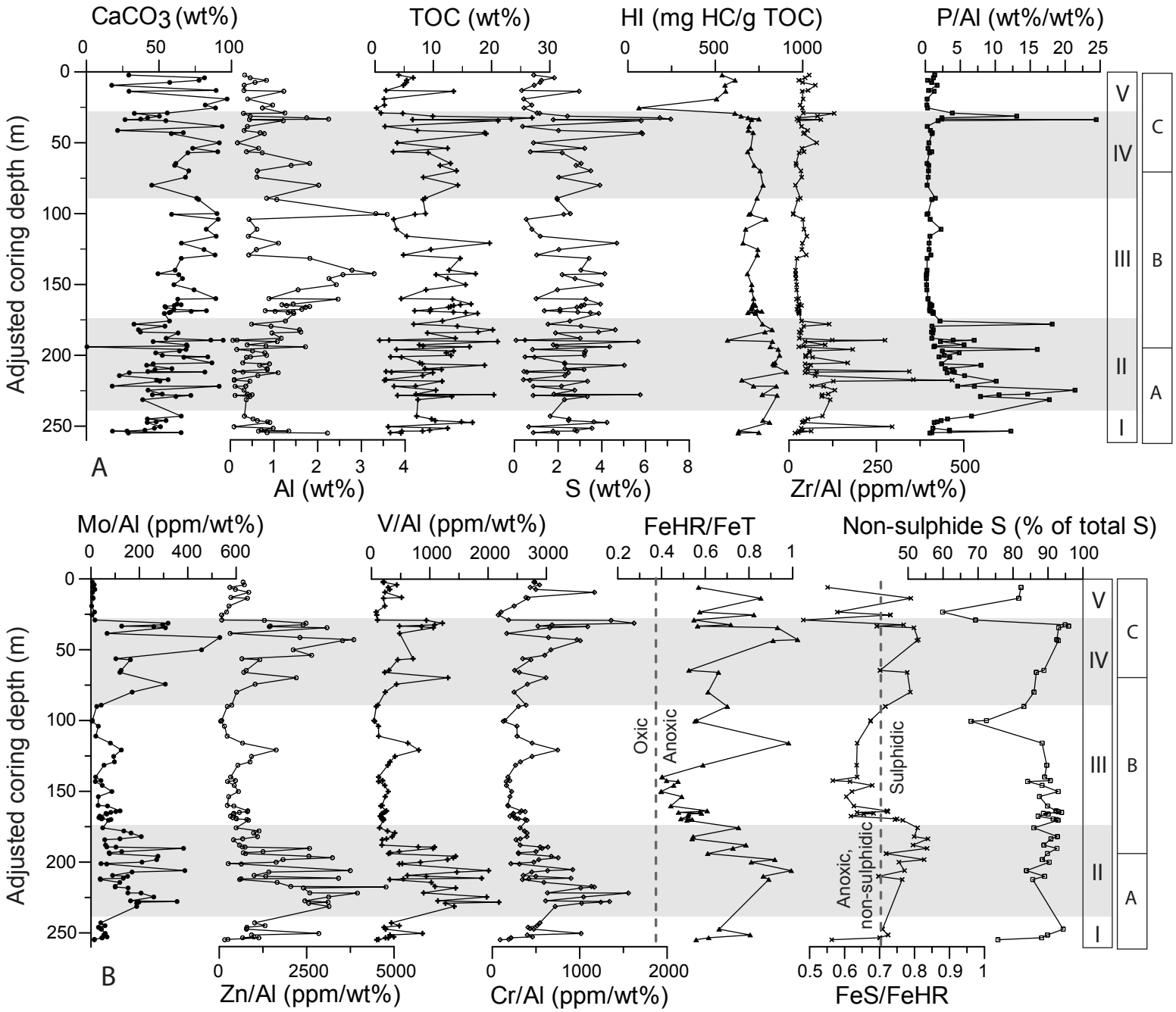

Figure 2

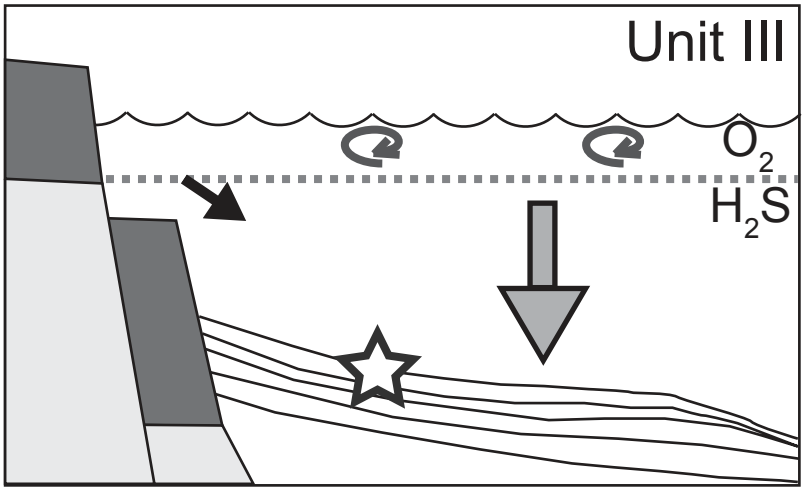

*Deposition below wave base
*Shallow redoxcline
*Anoxic/euxinic seafloor
*High primary productivity
*Moderate reworking of older sediments
*Reworked nannofossils

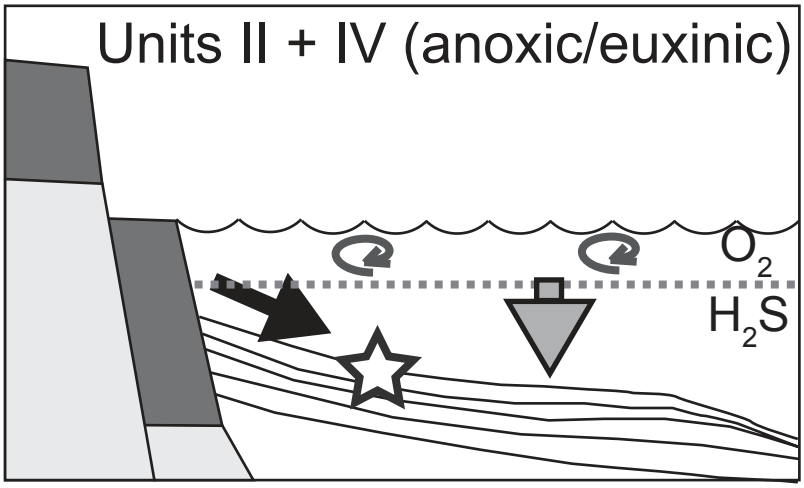

*Deposition below wave base
*Shallow redoxcline
*Anoxic/euxinic seafloor
*High primary productivity
*Intense OC + TM reworking
*Reworked nannofossils

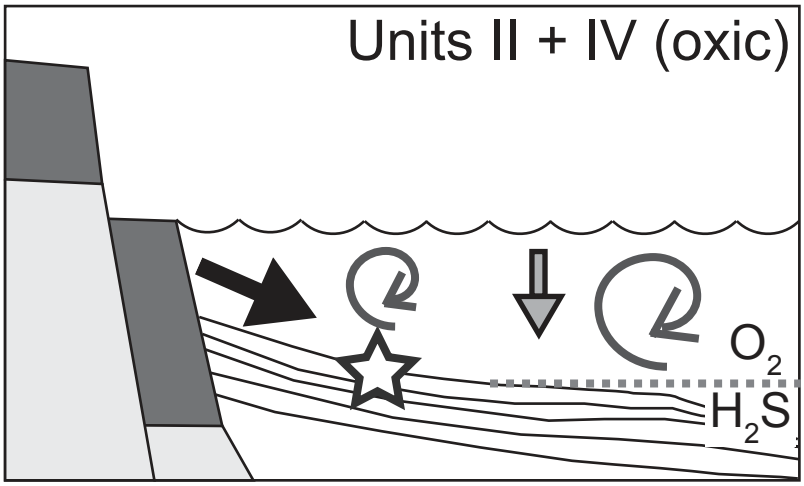

*Wave and/or current activity
*Deep redoxcline
*Oxic seafloor + bioturbation
*High primary productivity
*Intense OC + TM reworking
*Winnowing of nannofossils
*Heavy mineral enrichments

Figure 3

Table 1

	Unit I *(OS23 / OS22)*	*Unit II* *(OS23 / OS22)*	*Unit III* *(OS23 / OS22)*
Mo_{xs} *(ppm, mean)*	**31** / **31**	**97** / **104**	**110** / **76**
Cr_{xs} *(ppm, mean)*	**248** / **210**	**265** / **296**	**360** / **373**
V_{xs} *(ppm, mean)*	**202** / **186**	**608** / **501**	**356** / **274**
Zn_{xs} *(ppm, mean)*	**521** / **566**	**703** / **958**	**825** / **671**

Unit IV *(OS23 / OS22)*	*Unit V* *(OS23 / OS22)*	*Belqa Group* [1] *(shale)*	*Belqa Group* [1] *(limestone)*	*Black Sea* [2] *(Unit 2)*
401 / 272	**38 / 7**	**496**	**5**	**116**
514 / 490	**186 / 222**	**392**	**125**	**12**
1638 / 1044	**139 / 129**	**688**	**113**	**126**
1906 / 469	**165 / 254**	**4666**	**220**	**31**

Med. Sapropels[2]	*C/T Boundary (OAE 2)*[2]
104	**315**
69	**124**
457	**935**
51	**1997**

ARGUMENTS AGAINST HYDROTHERMAL OR EPIGENETIC METAL ENRICHMENTS IN THE JORDAN OIL SHALES

In sedimentary rocks, hyper-enrichments of a wide range of trace metals are often explained by the syn-genetic input of metal-rich hydrothermal solutions or brines into the contemporaneous sea water, or by the post-depositional (epigenetic) stratiform intrusion of metal-rich fluids into sedimentary formations. Here we will argue against a contribution of either of these processes to the trace metal hyper-enrichments in the studied Jordan oil shales.

Ruling out epigenetic enrichments:

- In the cores, no stratiform or strata-cutting metal-rich veins or layers are found, but the metal enrichments appear to be finely dispersed within the sediment.
- The organic matter is of low thermal maturity, implying that the sediments were not affected by post-depositional high-temperature overprint.
- Highest metal enrichments do not stand in any relationship to lowest carbonate contents, which implies that metal enrichments did not form in carbonate dissolution features.
- The classical epigenetic stratiform ore deposits are most strongly enriched in Zn, but also in Pb, and not substantially enriched in Cr and V. However, the Jordan oil shales lack significant Pb enrichments and are instead strongly enriched in Cr and V.
- Fossils (e.g., planktonic and benthic foraminifera, shell fragments) are generally well to moderately preserved with sharp boundaries, and show no signs of dissolution by acidic hydrothermal fluids.
- The sedimentary texture (e.g., bioturbation features, laminations) are pristine throughout the cores and do not show any signs of post-depositional overprint.

Ruling out syn-genetic hydrothermal enrichments:

- There are no signs of volcanic activity on the Eocene paleo-shelf of Jordan, and no signs of hydrothermal mounds, veins or pathways in older (Cretaceous-Paleocene) strata in the area that could have delivered metal-rich hydrothermal solutions.
- Highest trace metal enrichments occur in Units II and IV, where enrichments of Zr and P as well as sedimentary structures and bioturbation features indicate episodic water column mixing. These conditions are not conducive to the spreading of a hydrothermal plume or metal-rich brine, which would require stable salinity stratification.
- Spreading of metal-rich brines is not supported by the continuous presence, and good preservation, of planktonic and benthic fossils as well as bioturbation features that exclude the presence of hyper-saline brines loaded with dissolved or particulate metals at toxic levels.

FIGURE CAPTIONS SUPPLEMENTARY FIGURES

Figure DR1: Element excess contents relative to average shale composition (Wedepohl, 1971, 1991) for Jordan oil shales (average for Units I-V in cores OS22 and OS23) and various modern and ancient organic-rich lithologies deposited under anoxic/sulfidic conditions (data from Brumsack, 2006; Fleurance et al., 2013; Coveney and Glascock, 1989; Slack et al., 2015; Lehmann et al., 2007).

Figure DR2: Core OS22 records of (A) $CaCO_3$ (wt%), Al (wt%), TOC (wt%), S (wt%), P/Al (wt%/wt%), and Zr/Al (wt%/ppm); and (B) Mo/Al (ppm/wt%), Zn/Al (ppm/wt%), V/Al (ppm/wt%), Cr/Al (ppm/wt%), FeHR/FeT, FeS/FeHR and non-sulphide S (% of total S),

against adjusted drilling depth (meters, 0 m = top of black shale succession). Columns on right are geochemical Units (I-V) and lithological units (A-C).

Supplemental Figure 1

Click here to download Supplemental file Figure DR1 Excess.pdf

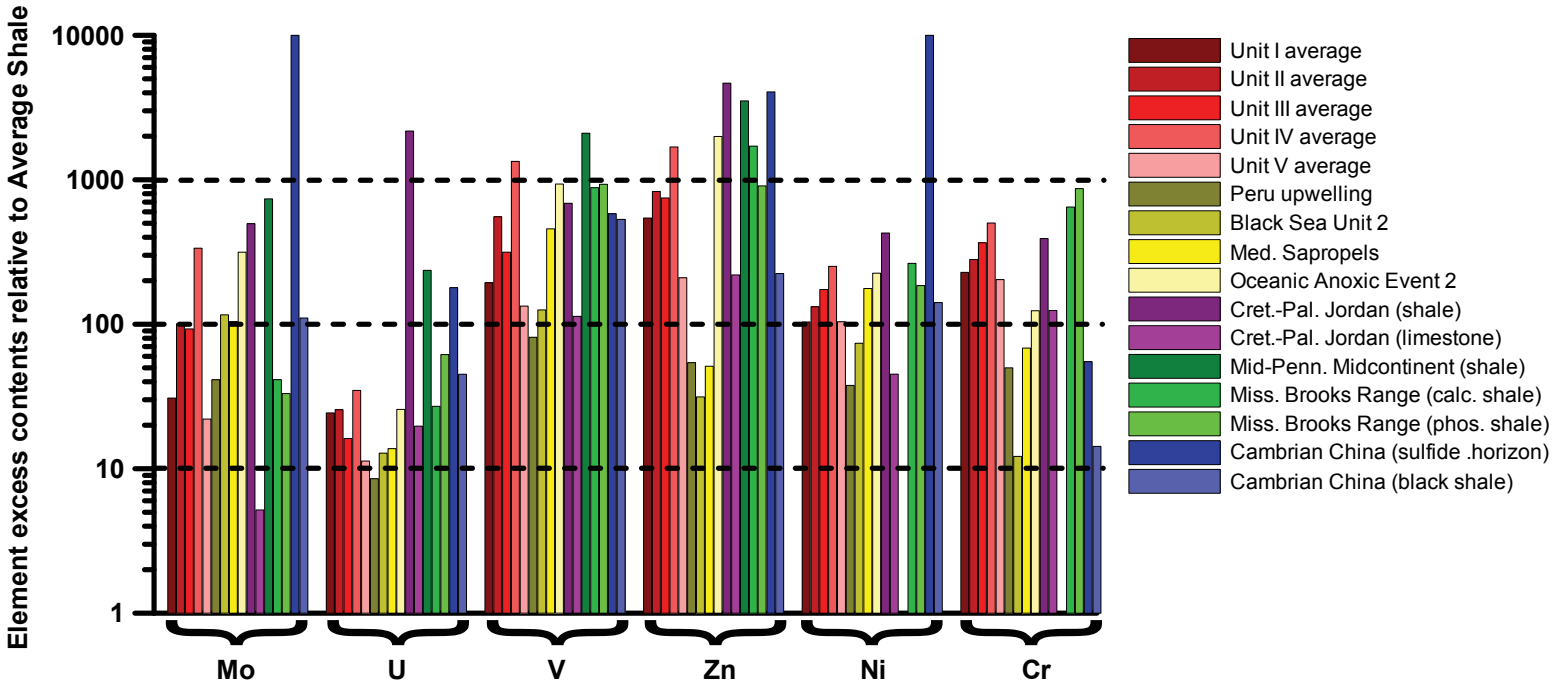

Figure DR1

Supplemental Figure 2

Click here to download Supplemental file Figure DR2.pdf

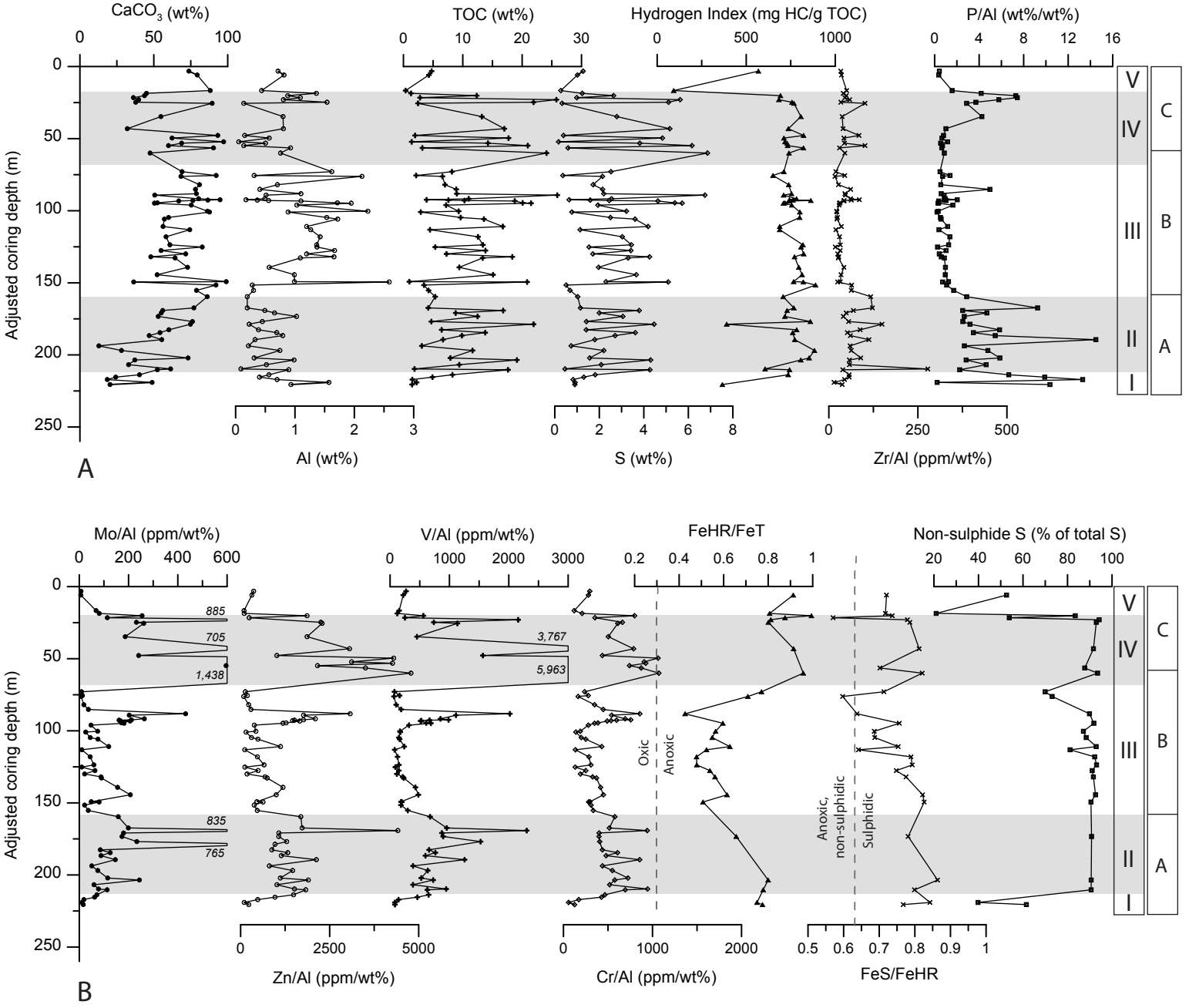

Figure DR2